Chinese Chemical Letters 34 (2023) 107909

Contents lists available at ScienceDirect

Chinese Chemical Letters

journal homepage: www.elsevier.com/locate/cclet

Clusteroluminescence: A gauge of molecular interaction

Bin Liu[a], Bo Chu[b], Lixun Zhu[d], Haoke Zhang[b,*], Wang-Zhang Yuan[c,*], Zheng Zhao[d,*], Wen-Ming Wan[e,*], Xing-Hong Zhang[b,*]

[a] School of Energy and Power Engineering, North University of China, Taiyuan 030051, China
[b] MOE Key Laboratory of Macromolecular Synthesis and Functionalization, Department of Polymer Science and Engineering, Zhejiang University, Hangzhou 310027, China
[c] School of Chemistry and Chemical Engineering, Frontiers Science Center for Transformative Molecules, Shanghai Key Lab of Electrical Insulation and Thermal Aging, Shanghai Electrochemical Energy Devices Research Center, Shanghai Jiao Tong University, Shanghai 200240, China
[d] School of Science and Engineering, The Chinese University of Hong Kong, Shenzhen 518172, China
[e] State Key Laboratory of Structural Chemistry, Key Laboratory of Coal to Ethylene Glycol and Its Related Technology, Center for Excellence in Molecular Synthesis, Fujian Institute of Research on the Structure of Matter, Chinese Academy of Sciences, Fuzhou 350002, China

ARTICLE INFO

Article history:
Received 5 September 2022
Revised 28 September 2022
Accepted 17 October 2022
Available online 19 October 2022

Keywords:
Clusteroluminescence
Clusterization-triggered emission
Through-space interaction
Non-conjugated structure

ABSTRACT

Clusteroluminescence (CL) materials, as an emerging class of luminescent materials with unique photophysical properties, have received increasing attention owing to their great theoretical significance and potential for biological applications. Although much progress has been made in the design, synthesis and application of CL materials, there is still a big challenge in the emission mechanism. So far, through-space interaction has been proposed as the preliminary mechanism of the corresponding clusterization-triggered emission (CTE) effect, but a systematic theory is still needed. This review summarizes the current mechanistic understanding of CL materials including organic/inorganic small molecules, and polymers with/without isolated aromatic structures. In addition, some strategies to achieve high quantum yield, adjustable emission color, and persistent room temperature phosphorescence in CL materials are also summarized. At last, a perspective of the mechanism and application of CL materials are demonstrated, which inspire the researchers working on the development of new kinds of functional materials.

1. Introduction

Luminescent materials have been systematically studied and widely applied in many areas such as display technology [1–3], cell imaging [4–7] and sensors [8–12]. Among the intensive and broad study of luminescence materials, more and more clusteroluminescence (CL) materials were discovered and concluded [13,14], which include natural or synthetic organic polymers [3,15–21], small molecules with nonconjugated structures [22,23], as well as inorganic complexes (or organic-inorganic hybridization) with metal core and heteroatomic surface ligands [24,25]. Unlike traditional π-conjugated molecules with aggregation-caused quenching (ACQ) or aggregation-induced emission (AIE) effects [26–29], there is no definite chromophore in the structure of CL molecules such as polyether [30], polyester [15], oligo(maleic anhydride) [17], poly(hydroxyurethane) [3], poly(amido amine)s [31] and amino acids [32]. And they usually exhibit some unique features such as non-conjugated structures, multiple emission peaks, unmatched absorption and excitation, excitation-dependent luminescence and room-temperature phosphorescence [33]. By performing and summarizing relative research in this area, Tang and coworkers proposed the theory of through-space interaction (TSI) to comprehensively explain the phenomenon of clusterization-triggered emission (CTE), which guide further expansions in organic CL study [34,35]. This theory effectively bridges the gap between traditional luminescent and "non-luminescent" materials and opens up a new field of luminescent materials.

The photophysical performances of luminogens with CL (CLgens) are manipulated by their structures and the mode of TSI (n-n, n-π and π-π) [33,36]. For example, some crystal sugars and amorphous polyols without even π electrons display variable PL and distinct persistent room temperature phosphorescence (p-RTP) [37,38], in which case the through-space n-n interactions from oxygen clusters dominate the CL. It is noteworthy that TSI is not a spontaneous process that requires an external driving force. Crystallization, hydrogen bond, coordination bond, ionic bond and polymerization are the widely reported methods for inducing TSI,

* Corresponding authors.
E-mail addresses: zhanghaoke@zju.edu.cn (H. Zhang), wzhyuan@sjtu.edu.cn (W.-Z. Yuan), zhaozheng@cuhk.edu.cn (Z. Zhao), wanwenming@fjirsm.ac.cn (W.-M. Wan), xhzhang@nuc.edu.cn (X.-H. Zhang).

https://doi.org/10.1016/j.cclet.2022.107909
1001-8417/

Table 1
Summary of similarities and differences of four CL materials.

	Organic small molecules	Inorganic small molecules	Polymers with isolated aromatic structures	Polymer without aromatic structures
Clear molecular arrangement [a]	√	√	×	×
Single crystal structure [a]	√	√	×	×
High crystallinity [b]	√	√	×	×
Excellent film-forming property [c]	×	×	√	√
Diversification of structure [d]	√	×	√	√
Biocompatibility [e]	√	√	×	√
Tunable molecular weight [f]	×	×	×	×

[a] A clear molecular arrangement can be obtained through the single crystal structure, which is beneficial to the study of TSI.
[b] High crystallinity can induce conformational rigidity and promote fluorescence and phosphorescence emission. However, the tunable crystallinity of some polymers is beneficial to study the effects of crystalline and amorphous on CL.
[c] Excellent film-forming properties make it a good substitute in the field of optoelectronic devices.
[d] The structural diversification of small organic molecules has important guiding significance for studying the influence of electronic and steric hindrance effects on TSI. For polymers, diverse polymer structures enrich the emission of luminescence, and hierarchical structures (such as configurations (isotactic, syndiotactic, atactic, *cis-trans* isomers), architectures (linear, star, crosslinked, hyperbranched, dendritic), sequences (alternating, block), conformation and aggregation (crystalline and amorphous states)) are conducive to the regulation of TSI and luminescent properties.
[e] Excellent biocompatibility makes them good candidates in the fields of cell imaging and drug delivery.
[f] The emission wavelength and QY can be regulated by the molecular weight of the polymer, exhibiting PIE characteristics. But the complex molecular structure of polymers (such as hierarchical structure and non-monodisperse molecular weight) also increases the difficulty of CTE research.

which are also effective strategies to regulate the photophysical properties of CL [39,40]. Although TSI among heteroatoms or heteroatoms-aromatic rings can explain the CL, direct experimental data to support these TSI interactions are still absent. Therefore, the chromophore determination, characterization and homologous mechanism study of CL are still challenging areas that deserved further exploration.

In this mini-review, we summarize the recent research progress of four typical CL materials, including organic small molecules, inorganic small molecules, polymers with isolated aromatic structures, and polymers without aromatic structures, aiming to use these four typical representatives to reveal the chromophores and mechanisms of CL. A general summary of the similarities and differences of these four CL materials to facilitate further investigation of CL mechanisms is presented in Table 1. It is expected that this review will draw more attention from researchers, thereby inspiring more thoughts on CL mechanisms and expanding the application areas of CL materials based on their unique molecular structures.

2. Molecules with CL behaviors

2.1. Organic small molecules

Organic small molecules are usually crystalline, and the arrangement of groups can be obtained by single crystal structure. Therefore, they are ideal candidates to disclose the CTE mechanism. During the past decades, cyclic anhydrides and imides have received increasing attention as model systems for studying luminescent mechanisms and properties of CLgens [16,17,34,41–43]. It is also noted that while different luminescent derivatives of anhydrides and imides were developed, the regulation of their photoluminescence (PL) is still challenging, presumably owing to the very preliminary understanding of the emissive mechanism. Fortunately, with continuous endeavors, researchers have found possible ways to modulate the PL of nonaromatic anhydrides and imides, including solvatochromism [16], copolymerization [44–46], base [47] or heat [48] treatment, and donor-acceptor interaction [49]. These achievements would inspire future creation of novel CLgens with tunable PL, and shed new light on the mechanistic understanding (Fig. 1a).

Apart from fluorescence from singlet exciton, phosphorescence from triplet exciton is also prevailing in CLgens [42,50]. For instance, different crystals of sugars (*e.g.*, D-Xyl, D-Fru and D-Gal, Fig. 1b) display variable PL and distinct p-RTP under varying UV irradiations (Fig. 1b) [37]. For anhydrides and imides, it is found that cryogenic phosphorescence, RTP and even p-RTP can be readily accessed in their aggregates, which might stem from the presence of carbonyl groups, heteroatoms, and the effective clustering of nonconventional chromophores [51–55]. Owing to the susceptibility of triplet exciton, phosphorescence can be facilely regulated. Meanwhile, since most aliphatic anhydrides and imides can generate fluorescence and phosphorescence emissions at the aggregate states, it is thus rational to tune their PL and phosphorescence (including PL efficiency (Φ), color, and phosphorescence lifetimes (τ_p)) through the change of excitation wavelength (λ_{ex}), temperature, microenvironment of the clusters, *etc.* Below we summarized several examples on the PL regulation of these CLgens.

Yuan *et al.* [51] reported the color-tunable p-RTP from the crystals of hydantoin (HA) and its 1,1′-methylenedihydantoin (MDHA) and 1,1′-(ethane-1,1-diyl)dihydantoin (EDHA) analogs (Fig. 1c). Concretely, sky-blue to yellowish-green p-RTP was observed from HA crystals with varying λ_{ex}s, with unprecedented PL and phosphorescence efficiencies (Φ_c and Φ_p) and τ_p of up to 87.5%, 21.8% and 1.74 s, respectively. Planar HA molecules interact with one another through multiple hydrogen bonds and other short contacts, which afford intense electronic communications and highly stiffened conformations, thus leading to efficient CL with noticeable tunability. Meanwhile, despite 5,5-dimethylhydantoin (MHA) crystals showing no p-RTP, tunable cryogenic phosphorescence afterglows can be obtained at 77 K, owing to the impeded molecular motions. Similarly, Yuan and coworkers further designed and synthesized highly twisted *N,N*′-carbonylbissuccinimide (CBSI) and *N,N*′-oxalylbissuccinimide (OBSI) comprising multiple carbonyls and imide units, which demonstrate tunable PL and p-RTP in response to λ_{ex} (Fig. 1d) [52]. The concurrence of diverse luminescent species is responsible for such tunable emissions. Calculations for monomers to tetramers of both compounds suggest the effective TSI in crystals (Fig. 1d), which varies in diverse clusters, thereby generating λ_{ex}-dependent PL and p-RTP [52].

Other than excitation sources, Yuan *et al.* demonstrated the feasibility of PL modulation of nonaromatic anhydrides and imides through internal and external regulations [53]. Mutual bridging of isolated subgroups by an electron-rich unit effectively promotes intramolecular TSI, resulting in red-shifted and enhanced emission with prolonged p-RTP. Meanwhile, the replacement of oxygen by nitrogen remarkably changes the TSI and significantly enhances intermolecular interactions including the generation of hydrogen bonds, consequently, affording boosted Φ_c and Φ_p (Fig. 2a). Notably, upon freezing, compression, or embedding into poly-

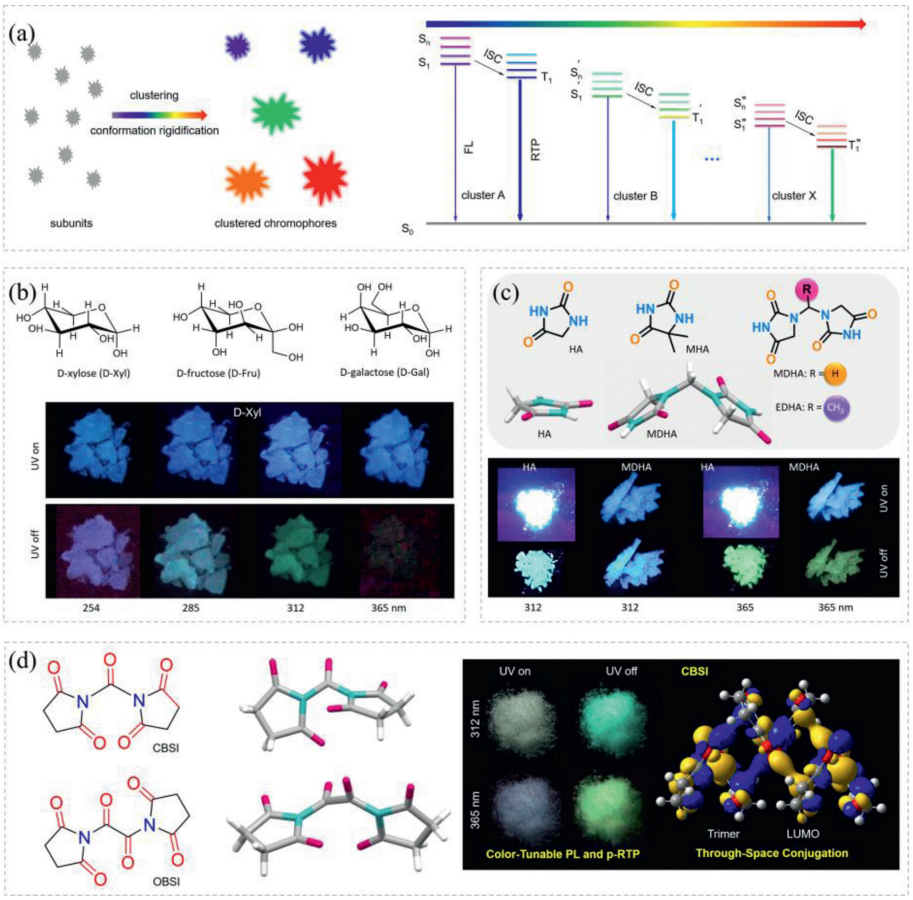

Fig. 1. (a) Illustration of the CTE mechanism and the generation of diversified emissive species of CLgens. (b) Chemical structures of D-Xyl, D-Fru and D-Gal and photographs of D-Xyl single crystals taken under or after the stop of different UV irradiations. Reproduced with permission [37]. Copyright 2020, the Royal Society of Chemistry. (c) Chemical structures of HA, MHA, MDHA and EDHA and photographs of HA and MDHA single crystals taken under or after ceasing 312 and 365 nm UV lights. Reproduced with permission [51]. Copyright 2020, the Royal Society of Chemistry. (d) Chemical and single crystal structures of CBSI and OBSI, photographs of CBSI single crystals taken under or after ceasing 312 and 365 nm UV lights, and electron density of the LUMO level of the CBSI trimer. Reproduced with permission [52]. Copyright 2020, the Wiley-VCH GmbH.

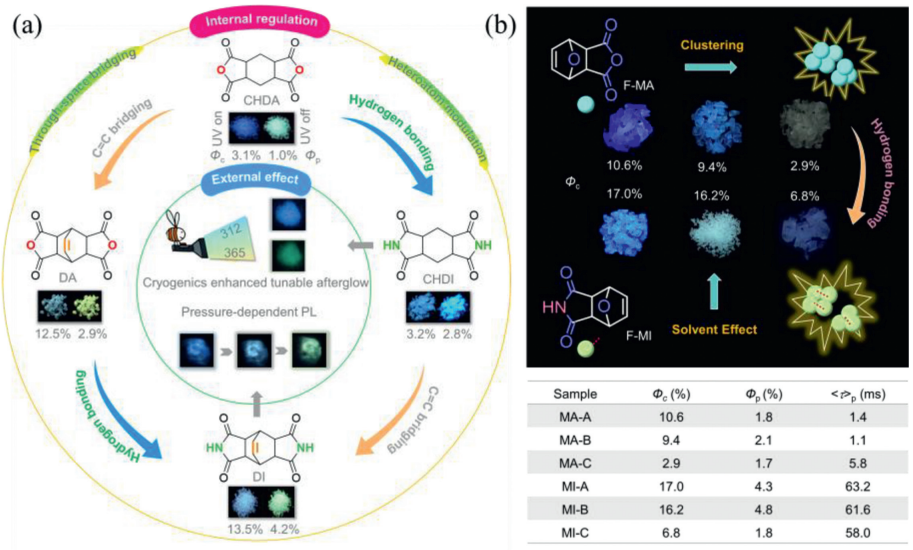

Sample	Φ_c (%)	Φ_p (%)	$\langle\tau_p\rangle$ (ms)
MA-A	10.6	1.8	1.4
MA-B	9.4	2.1	1.1
MA-C	2.9	1.7	5.8
MI-A	17.0	4.3	63.2
MI-B	16.2	4.8	61.6
MI-C	6.8	1.8	58.0

Fig. 2. (a) Internal and external strategies towards PL regulation of CLgens. Copied with permission [53]. Copyright 2020, the Wiley-VCH GmbH. (b) Polymorphism dependent PL of F-MA and F-MI crystals. Copied with permission [54]. Copyright 2021, the SIOC.

mer matrices, the PL intensity and color of the aggregates can also be well regulated [53]. Based on these results, Yuan and coworkers further cultured single crystals of furan-protected maleic anhydride (F-MA) and furan-protected maleimide (F-MI) in different solvents. Interestingly, polymorphs of both compounds were acquired with distinct PL colors and RTP (Fig. 2b) [54]. Under 312 nm UV light, three polymorphs of F-MA (MA-A∼C) exhibit bluish-violet, blue, and white light emissions with variable Φ_c and Φ_p values. F-MI polymorphs (MI-A∼C) with effective hydrogen bonding also display tunable emissions with strikingly improved PL performance with comparison to those of F-MA crystals. It is found that residual trace solvents in crystals bring about small changes in molecular conformations and packing modes of F-MA and F-MI, but exert significant impact on intra/intermolecular interactions of the emissive clusters. Consequently, the relative intensity of singlet (fluorescence) and triplet (RTP) is changed, thus resulting in polymorphism-dependent PL.

Besides the above strategies, very recently, they reported the impressive red and near infrared (NIR) RTP emissions from small nonaromatic cyclic imides through synergistic effects of molecular clustering, π-π stacking and halogen effects [55]. Meanwhile, while polymaleimides (PM) obtained by free radical polymerization (Fr-PM) generally depict blue emission, Zhang's group [56] showed the facile and effective tuning on the PL of PM through anion polymerization (A-PM). Full color emissions of A-PM solids were realized through the change of the Lewis base catalysts. These findings not only provide deeper understanding on the luminescent mechanism, but also pave the way to the promising technical applications in bioimaging, sensing, encryption, and so forth.

2.2. Inorganic small molecules

In comparison with organic species, inorganic complexes with luminescence properties were discovered even earlier and some inorganic complexes or organometallic compounds also exhibit similar CL phenomenon [24,25]. Since the inorganic complexes or organometallic compounds are much easier to crystallize, they may work as excellent model compounds to elucidate the chromophore formation process and unveil the structure-property relationship of CL system.

Zhao *et al.* investigated the mechanism of an ancient inorganic AIE system using platinocyanide complexes and mainly concluded the luminescence mechanism from three aspects [25]: (1) Aggregation of $BaPt(CN)_4$ can be triggered by high fraction (99%) of poor solvent (THF) or low temperature (77 K), which generated chromophores with large cluster structures and gave strong intermolecular interactions between Pt ions to emit strong fluorescence (Fig. 3a); (2) Switching counter ions ($BaPt(CN)_4\cdot 4H_2O$, $K_2Pt(CN)_4\cdot 3H_2O$, and $Na_2Pt(CN)_4\cdot 3H_2O$) introduced varying intermolecular interaction and modified the size of chromophores, which also resulted in variable emission wavelength and quantum yield (QY) (Fig. 3b); (3) Structural rigidity affected the luminescence property largely, which was proved by comparing QY of pristine crystal and ground powder (Fig. 3c). The results suggested that the formation of chromophores involved interconnections between planar square $Pt(CN)_4^{2-}$ to generate columnar channel, which promoted charge transfer and energy splitting of platinum d orbitals, and brought out the visible emission from the strong Pt-Pt interactions. Concentrations, counter ions, and coordinative H_2O molecules of the platinocyanide system were taken into concern for the distance between platinum cores and the metal complex rigidity, as shown in Fig. 3d, which alternated the luminescence properties from multiple aspects since they can affect the nonradiative decay of the excited state.

Another research performed on a phosphorescent gold(I) complex, which emits white light phosphorescence (Fig. 4a), was reported in 2021 [24]. The gold(I) complex, $[(CF_3Ph)_3PAuC{\equiv}CPh]$ (TPPGPA), was discovered in dichloromethane (DCM) to have monomeric (Fig. 4b inset) and trimeric structure (Fig. 4c), which corresponds to the metal-perturbed $^3\pi\pi^*$ intracomplex charge transfer (^{3}LLCT) endowed T_1 state and ligand-to-metal–metal charge-transfer (^{3}LMMCT) caused low-lying T_1' state, through the intersystem crossing from the S_1 state, as shown in Fig. 4d. Au-Au bond formation in the trimeric gold(I) complex was corroborated as the compulsory condition for new chromophore formation since it assisted the molecular packing and correlated with the emission wavelength and intensity. Mechanical grinding and temperature tests were performed on the gold complex, resulting in the elimination and redshift of long-wavelength peak respectively (Fig. 4e), which indicated that the aurophilic interaction induced trimer configuration was the dominant factor corresponding to the long-wavelength emission chromophore constitution.

Concluding from the discussed metal complex CL materials, the mechanism implied that new chromophore formation was dependent on the metal-metal interactions of corresponding metal cores, while the QY, emission wavelength, and lifetime more rely on the counter ions and complex rigidity. Current hot topics in inorganic luminescence materials including perovskite materials, metal-organic frameworks (MOF), and carbon quantum dots are designed based on the mechanism of quantum confinement effect, which mainly involves the mechanism of size adjustment and electron transferring ability. By solely based on the quantum confinement effect, it is incapable of explaining all the CL phenomena. Related researches in this area also proposed mechanisms involving nanoscale carbonyl clusters composed by carboxylate ligands and metal cores as chromophores [57], luminescence enhancement through the interaction between newly introduced metal ions and cluster cores [58], self-assembly nanoribbons through aurophilic interactions to generate significant luminescence enhancement [59], switchable fluorescence emission adjusted by guest molecules of MOF [60], and so forth. Through the numerous CL mechanisms summarized above, new perspectives and conclusive theories should be developed to help systematically understand more thoroughly on both organic and inorganic CL materials.

2.3. Polymers with isolated aromatic structures

Compared to small molecules, CL polymers also play important roles in luminescent materials, attributed to their outstanding properties such as processing, film-forming and self-assembly. Recently, polymerization-induced emission (PIE) strategy has been proposed as an effective polymerization method for the molecular design of CL polymers from non-emissive monomers, where the constructions of both polymer chain and polymeric luminogens are realized simultaneously [39,61–68].

In 2017, Wan *et al.* successfully introduced the Barbier reaction into polymer chemistry as a Barbier polymerization method for the molecular design of a series of CL poly(phenylalcohol)s [61]. They discovered monomer structure and polymerization time-dependent untraditional luminescence from non-emissive monomers and therefore proposed PIE strategy in 2019 (Fig. 5) [62]. Recently, Barbier polymerization has been realized through A_2+B_2, AB, AB_2 and A_2+B types of one-pot polyadditions of different C=O containing compounds including ketones, esters, amides and peroxyester [61–68]. Interestingly, the luminescence type can be easily tuned from AIE and ACQ by Barbier polymerization. Taking linear poly(phenylmethanol)s as examples, phenylmethanol moieties (*e.g.*, triphenylmethanol) contain sp^3 hybridized carbon center, which limits the extension of π system and results in non/weak luminescence. However, when triphenylmethanol moiety is incorporated in polymer chain through polymerization (*e.g.*, Barbier polymer-

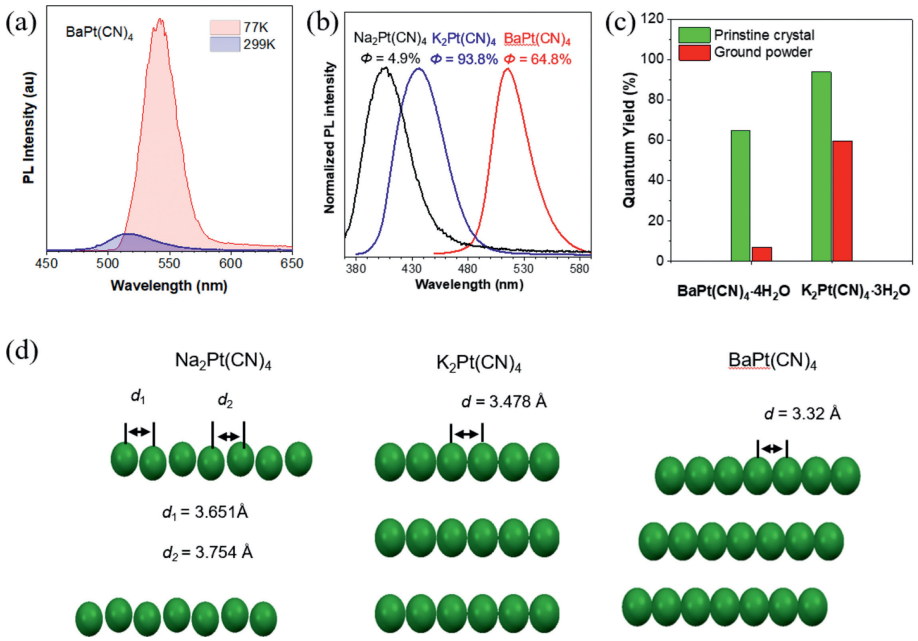

Fig. 3. (a) PL spectrum for $BaPt(CN)_4 \cdot 4H_2O$ at 77 K and 299 K. (b) PL spectra and QYs of the crystals of $BaPt(CN)_4 \cdot 4H_2O$, $K_2Pt(CN)_4 \cdot 3H_2O$, and $Na_2Pt(CN)_4 \cdot 3H_2O$. (c) QYs of pristine crystal and ground powder of $BaPt(CN)_4 \cdot 4H_2O$ and $K_2Pt(CN)_4 \cdot 3H_2O$ measured by an integrating sphere; λ_{ex}: 365 nm. (d) Intermolecular Pt-Pt distances in the single crystals of $BaPt(CN)_4 \cdot 4H_2O$, $K_2Pt(CN)_4 \cdot 3H_2O$, and $Na_2Pt(CN)_4 \cdot 3H_2O$. Reproduced with permission [25]. Copyright 2021, the Wiley-VCH GmbH.

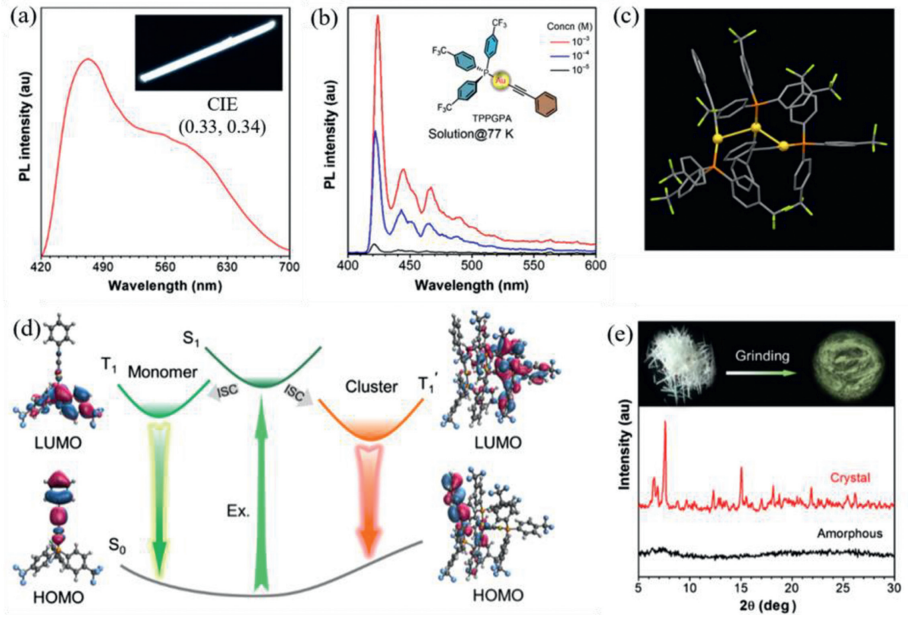

Fig. 4. (a) PL spectrum of crystalline TPPGPA. Inset: PL image taken at $\lambda_{ex} = 360$ nm. (b) PL spectra of monomeric TPPGPA in DCM solution with different concentrations at 77 K. The inset in (b) shows the structure of TPPGPA. (c) The molecular structure of trimeric TPPGPA with 50% probability ellipsoids. Hydrogen atoms were omitted for clarity. (d) Electron cloud distributions of TPPGPA monomer (gas state) and trimer (solid-state) in the ground state at the TD-DFT B3LYP/(6–31G**+LANL2DZ) level and the schematic illustration of emission from triplet state of the crystalline TPPGPA. (e) PXRD patterns of TPPGPA in crystalline and amorphous states, and an image of the solid sample of TPPGPA taken under UV irradiation before and after mechanical grinding. Reproduced with permission [24]. Copyright 2021, the Chinese Chemical Society.

ization), TSI and intramolecular charge transfer effect can be induced under the constraint of polymer chains, resulting in PIE. When substitutions of poly(phenylmethanol) contain alkyl group, it is weakly luminescent. When all substituents are phenyl rings, poly(triphenylmethanol)s are luminescent. When all phenyl groups of poly(triphenylmethanol)s are rotatable, they are AIE-type luminescence. When some phenyl groups of poly(triphenylmethanol)s are rotation forbidden, they are ACQ type luminescence. This connection mode-dependent PIE is similar to the theory of restriction of intramolecular motion (RIM). In the Barbier hyperbranched polymerization, PIE is not only connection mode dependent, but also polymerization time dependent. Taking the AB_2 type Barbier hyperbranching polymerization of 4,4′-dichlorobenzophenone as an example, both solution and solid state of polymerization media are weakly luminescent before polymerization. With the increase of polymerization time from 15 min to 4 h, 12 h and 24 h, the polymerization media starts to emit blue, cyan, green, and yellow colors in the solid state while the solution state is still weakly luminescent, which is typical PIE-active. Both poly(triphenylmethanol)s and poly(triphenylethanol)s exhibit

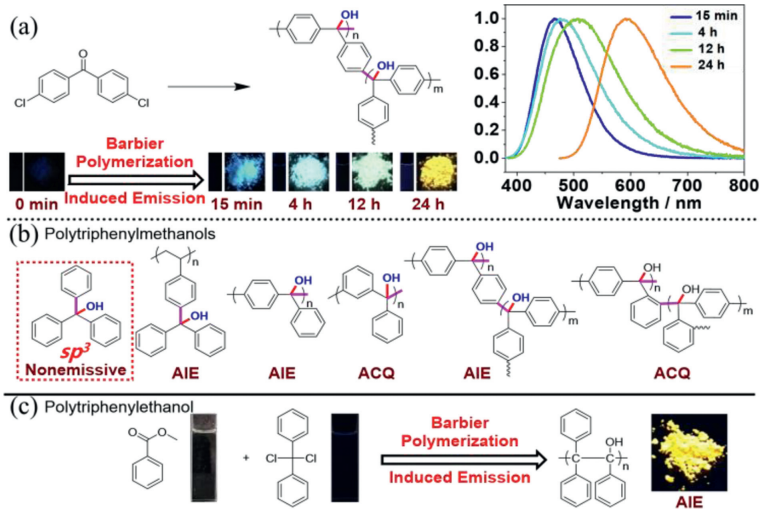

Fig. 5. CL polymers prepared through Barbier PIE. (a) Barbier hyperbranching polymerization exhibiting polymerization time dependent PIE. Reproduced with permission [62]. Copyright 2019, the American Chemical Society. (b) Typical polytriphenylmethanols exhibiting PIE. (c) Polytriphenylethanol prepared through A2+B type Barbier polymerization. Reproduced with permission [63]. Copyright 2020, the Elsevier.

PIE, which can be prepared through A_2+B type Barbier polymerization of dichlorodiphenylmethane and benzoate. Different from linear *para*-poly(triphenylmethanol) with cyan color, linear poly(triphenylethanol) exhibits yellow color. It is worth mentioning that there are plenty of commercially available monomers that are suitable for Barbier polymerization. All of these indicate nonconjugated luminescence color can be easily adjusted through Barbier PIE, by adjusting wildly available commercial monomers, which might cause the inspiration for the molecular design and applications of CL polymers including CL.

At the same time, Zhang *et al.* proposed a PIE concept on the basis of summarizing a large number of CL polymers, and proposed two major characteristics of PIE [39]: (1) The wavelength and intensity of PL depend on the degree of polymerization of polymers, which is the basic condition for the formation of clusters; (2) A diverse polymer structure (such as configurations, architectures, sequences, conformation, and aggregation) enriches the emission of luminescence. Finally, to distinguish it from other fields and study the properties of CL more conveniently, clusters are defined by Liu and coworkers, that is, clusters are the basic emission units, which are formed by the aggregation of electron-rich groups, thereby generating delocalized electrons and further inducing emission.

2.4. Polymer without aromatic structures

Compared to CL polymers with aromatic structures, CL polymers without benzene ring structures attracted more attention owing to their excellent solubility, biocompatibility, and film-forming properties. Currently, structural regulating of CLgens focuses on the primary structure of various groups such as ethers [30], amides [3,19] and esters [15–17], although hierarchical structures of CLgens such as proteins play a more important role in manipulating the TSI [69,70]. Meanwhile, the CL is mostly focused on dominant blue-light emission with low QY and display excitation-dependent emission, which may originate from the subgroups, such as radiative n-π^* transition of carbonyl groups in polyesters and polypeptides [71–73]. Remarkably, due to the TSI nature, CLgens always show multiple emission peaks, which is the best candidate to construct long-wavelength emission or even white-light emission [2,74]. Compared with crosslinking and branched polymers, linear polymers with single heteroatom groups may be good candidates to verify cluster structures, the formation of clusters and the mechanism of CL, meanwhile, regulating hierarchical structures can build the relationship between clustering structures and TSI to achieve the long-wavelength and high-efficiency CL materials.

Zhang *et al.* reported a linear non-conjugated polyester exhibiting yellow-green CL and a high QY of 38% [15]. All the polyesters P1-P4 showed short-wavelength emission with PL peaks at 440 nm in DCM, which originated from the n-π^* electron transition of ester groups *via* theoretical calculations. In addition to the short-wavelength emission peak at 440 nm, P3 also displayed a long-wavelength emission peak at 530 nm with excitation-independent emission (Fig. 6a). Combined with the enhancement effect on the absorption band at 300–350 nm of n-π^* transition related to the special aggregate structures of carbonyl groups, the long-wavelength emission (530 nm) of P3 were identified from the ester clusters. Meanwhile, in Figs. 6b and c, the concentration-dependent PL and QY curves not only showed AIE effect, but also visualized the formation of clustering: one is cluster formation and increase in cluster amount below the critical concentration at 10^{-3} mol/L, and the other is the growth of cluster numbers over 10^{-3} mol/L. More importantly, the dynamic characteristics of clusters were also verified by temperature-dependent PL curves in concentrated solutions (Fig. 6d). The intensity of PL was firstly weakened and the peaks shifted from 515 to 470 nm with elevating the temperature from 10 °C to 60 °C, then remains nearly unchanged from 60 °C to 80 °C except for reduced PL intensity. Interestingly, the PL spectra can gradually return to the original one with decreasing temperature from 80 °C to 10 °C. In this work, the crucial rule that primary structure with balanced flexibility and rigidity endowed P3 the longest CL wavelength and highest QY was further discovered (Fig. 6e).

After that, Zhang *et al.* further reported a linear nonconjugated polyester with single molecular white-light emission (SMWLE) by regulating the hierarchical structures of aliphatic polyesters, which build the relationship between hierarchical structures and TSI experimentally [75]. In Fig. 7a, PL spectra of P2 in DCM showed a clear excitation-dependent emission effect with the transformation from dominant short-wavelength emission (~460 nm) of n-π^* transition of carbonyls to negligible long-wavelength emission (~540 nm) of ester clusters. After introducing rigid double bonds into polyesters, trans-alkene based P10 showed a stronger emission peak at ~540 nm in DCM solution owing to more stable clusters (Fig. 7b). When transformation from *trans*-alkenes to *cis*-alkenes,

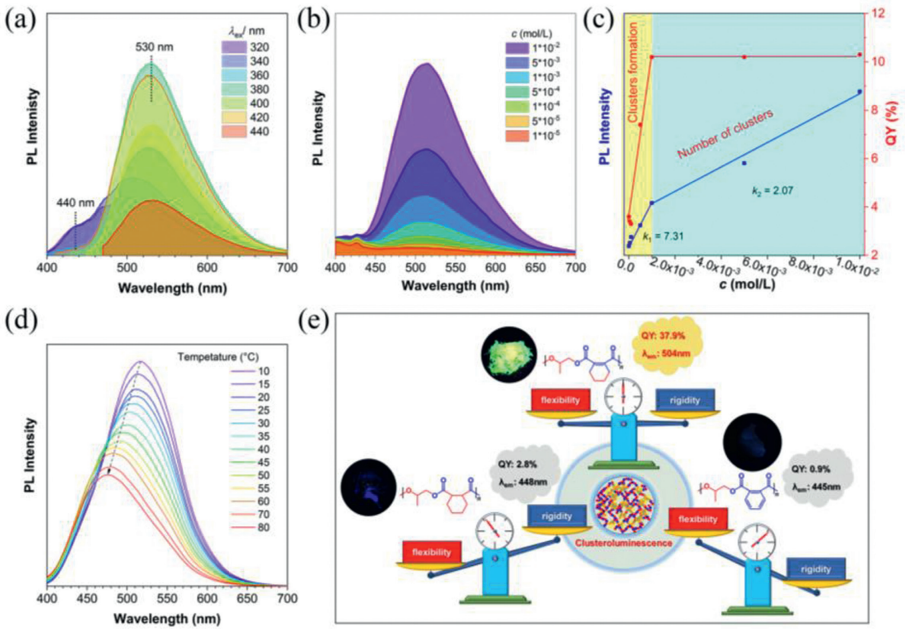

Fig. 6. (a) PL spectra ($c = 10^{-3}$ mol/L) of P3 in DCM. (b) Concentration-dependent PL spectra of P3 in DCM. (c) Plots of PL intensity and QY *versus* concentration for P3 in DCM. (d) Plots of PL intensity *versus* temperature in dimethylformamide ($c = 0.1$ mol/L), $\lambda_{ex} = 400$ nm. (e) Summarized photophysical data of P1, P3 and P4 from left to right dependent on the balance of rigidity and flexibility. Inset: photographs of P1, P3 and P4 from left to right taken under 365 nm UV light. Reproduced with permission [15]. Copyright 2022, the Wiley-VCH GmbH.

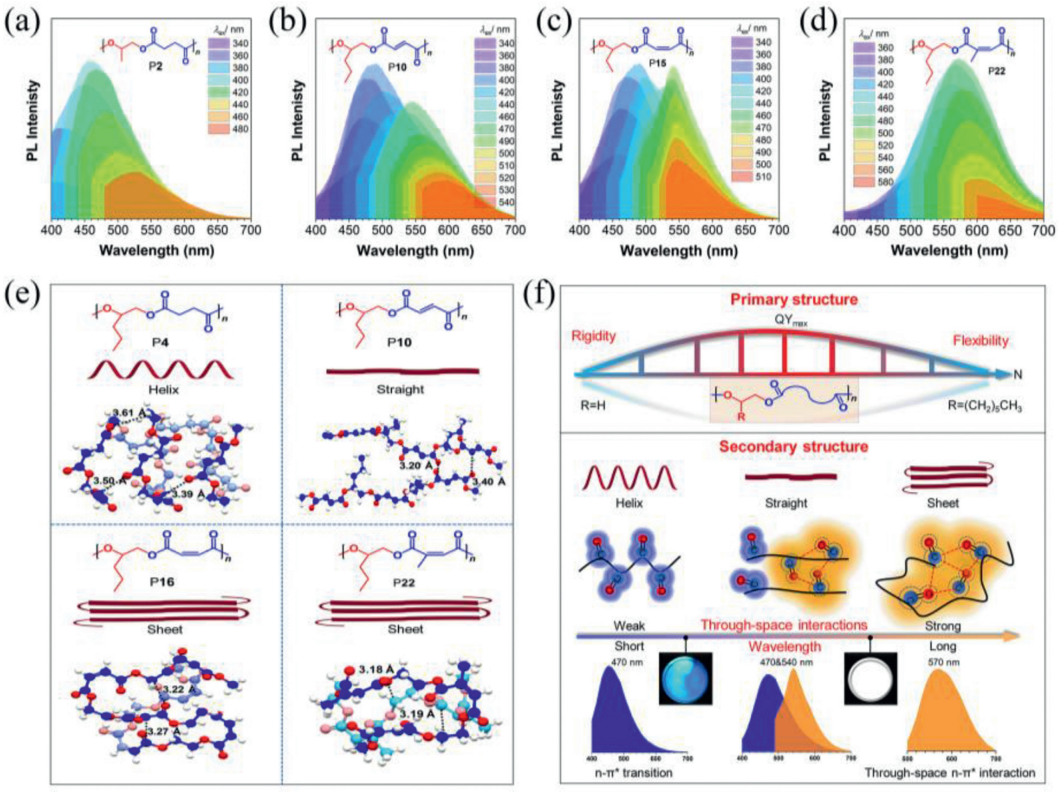

Fig. 7. PL spectra ($c = 10^{-3}$ mol/L) of (a) P2, (b) P10, (c) P15 and (d) P22 in DCM. (e) Theoretical calculations based on P4, P10, P16 and P22 with five constitutional units calculated by (TD-DFT) B3LYP/6–31(d) method. Black dotted lines represent the interchain or intrachain distance ($d_{O\cdots C}$) between carbon and oxygen atoms with the participation of the carbonyl group. (f) Effects of primary structure and secondary structure on photophysical properties of aliphatic polyesters, respectively. Red dotted lines represent the TSI. Reproduced with permission [75]. Copyright 2022, the American Chemical Society.

in Fig. 7c, the CL peaks at 540 was further increased, which is equal to that at 470 nm. Once methyl group was introduced into the *cis*-alkenes to serve as the anchor (Fig. 7d), the CL peak directly shifted to 570 nm, which is the longest for nonconjugated aliphatic polyesters reported so far. Obviously, the enhanced and red-shift CL at 540–570 nm suggested that TSI was continuously boosted. To figure it out, this work disclosed that the inner changes of secondary structures induced the boosted TSI theoretically and experimentally (Figs. 7e and f). P4 possessed helix conformation with $d_{O\cdots C}$ in the range of 3.39–3.61 Å beyond the sum of their van der Waals radii, which had negligible through-space n-π interaction and only showed short-wavelength CL around 460 nm. Replacement by trans-alkenes, the resultant P10 showed nearly regular, straight conformation with interchain $d_{O\cdots C}$ in the range of 3.2–3.4 Å, inducing a strong interchain through-space n-π interaction with long-wavelength CL at 540 nm. Interestingly, *cis*-alkene P16 exhibited folded sheet with short $d_{O\cdots C}$ in the range of 3.22–3.27 Å, which further intensifies the long-wavelength CL due to strong intrachain through-space n-π interaction. Moreover, adding the anchor of a methyl group into *cis*-alkenes further stabilized the folded sheet conformation with shorter $d_{O\cdots C}$ ($\sim$3.18 Å) and sharply enhanced the interchain through-space n-π interaction. Finally, P22 showed dominated and redder CL at 570 nm. It is noteworthy that P19 and P20, especially for P20, presented pure white-light emission with CIE coordination of (0.30, 0.32) based on the overlapped short-wavelength and long-wavelength CL (Fig. 7e). Also, this work disclosed that structural equilibrium of flexibility and rigidity only achieved highest QYs without PL change at primary structural level.

The above works have verified ester clusters with dynamic characteristics and achieved white to orange-light emission, which indicated that CL has the potential to be tuned into red-light emission, suggesting that regulating primary and secondary structures of aliphatic polyesters deeply embodies the philosophy of PIE [39,62]. In the field of CL, clusters with single heteroatom groups from simple synthetic chemistry may be good candidates to study CL, At present, blue-light emission and clear excitation-dependent emission may be caused by the unstable clusters and weak TSI, then the intrinsic emission of subunits are dominant [75]. So, manipulation of the hierarchical structures for polymers is one of the important directions in CL.

3. Conclusion and perspectives

In the past two decades, materials with CL properties have been widely studied and plenty of CLgens have been developed, including the above-mentioned organic and inorganic small molecules, and polymers with and without isolated aromatic structures. However, there are two thorny issues in this area: unclear emission mechanisms and dissatisfactory photophysical performances. Although researchers have devoted tremendous efforts to drawing the mechanistic picture for CTE from both the experimental and theoretical aspects, a systematic and comprehensive aggregate photophysics based on TSI is still absent, which is mainly caused by the uncertain structures, especially for polymer systems. Undoubtedly, building a clear structure-property relationship for CL is the basis of establishing aggregate photophysics. It is foreseeable that constructing models for CLgens to further clarify the involved TSI will be an important topic for the mechanistic study of CL. Besides, the short-wavelength emission and low luminescent efficiency are still problems for the utilization of CLgens. To overcome these drawbacks, physical or chemical crosslinking of subunits in CLgens will be one of the effective strategies, which is similar to the crosslinked polymer dots but with clear structures. In other words, future research should focus on the enhancement of TSI in CLgens *via* hierarchically structural modification. It is expected that the mechanistic study and improvement of photophysical performances for CL will pave the way for the practical applications of CLgens.

Declaration of competing interest

We declare that we do not have any commercial or associative interest that represents a conflict of interest in connection with the work submitted.

Acknowledgments

B. Liu thanks the support of the National Natural Science Foundation of China (No. 52003254). H. Zhang thanks the support from the Fundamental Research Funds for the Central Universities (No. 2021QNA4032), the Open Fund of Guangdong Provincial Key Laboratory of Luminescence from Molecular Aggregates, and South China University of Technology (No. 2019B030301003). Z. Zhao thanks the support of Shenzhen Key laboratory of Functional Aggregate Materials (No. ZDSYS20211021111400001), the Science and Technology Plan of Shenzhen (Nos. JCYJ2021324134613038 and GJHZ20210705141810031). W.Z. Yuan thanks the support of the National Natural Science Foundation of China (No. 52073172). X.-H. Zhang gratefully acknowledges the financial support of the National Science Foundation of the People's Republic of China (Nos. 51973190 and 21774108) and Zhejiang Provincial Department of Science and Technology (No. 2020R52006).

References

[1] L. Yu, C. Yang, J. Mater. Chem. C 9 (2021) 17265–17286.
[2] B. Liu, B. Chu, Y.L. Wang, Z. Chen, X.H. Zhang, Adv. Opt. Mater. 8 (2020) 1902176.
[3] B. Liu, Y.L. Wang, W. Bai, et al., J. Mater. Chem. C 5 (2017) 4892–4898.
[4] L. Shao, K. Wan, H. Wang, et al., Biomater. Sci. 7 (2019) 3016–3024.
[5] C. Xu, R. Guan, D. Cao, et al., Talanta 206 (2020) 120232.
[6] C. Weng, N. Fan, T. Xu, et al., Chin. Chem. Lett. 31 (2020) 1490–1498.
[7] D. Li, P.P. Sun, J.G. Li, et al., Acta Polym. Sin. 53 (2022) 856–873.
[8] Y. Shu, Q. Ye, T. Dai, Q. Xu, X. Hu, ACS Sens. 6 (2021) 641–658.
[9] Z. Zhao, X. Chen, Q. Wang, et al., Polym. Chem. 10 (2019) 3639–3646.
[10] B. Zhao, S. Yang, X. Yong, J. Deng, ACS Appl. Mater. Interfaces 13 (2021) 59320–59328.
[11] Q. Xiao, X. Zhao, H. Xiong, Chin. Chem. Lett. 32 (2021) 1687–1690.
[12] S. Jiang, L. Meng, W. Ma, et al., Chin. Chem. Lett. 32 (2021) 1037–1040.
[13] D.A. Tomalia, B. Klajnert-Maculewicz, K.A.M. Johnson, et al., Prog. Polym. Sci. 90 (2019) 35–117.
[14] Y. Zhang, P. Shen, B. He, et al., Polym. Chem. 9 (2018) 558–564.
[15] B. Chu, H. Zhang, L. Hu, et al., Angew. Chem. Int. Ed. 61 (2022) e202114117.
[16] E. Zhao, J.W.Y. Lam, L. Meng, et al., Macromolecules 48 (2015) 64–71.
[17] X. Zhou, W. Luo, H. Nie, et al., J. Mater. Chem. C 5 (2017) 4775–4779.
[18] C.L. Larson, S.A. Tucker, Appl. Spectrosc. 55 (2001) 679–683.
[19] Q. Wang, X. Dou, X. Chen, et al., Angew. Chem. Int. Ed. 131 (2019) 12797–12803.
[20] X. Dou, Q. Zhou, X. Chen, et al., Biomacromolecules 19 (2018) 2014–2022.
[21] L.L. Du, B.L. Jiang, X.H. Chen, et al., Chin. J. Polym. Sci. 37 (2019) 409–415.
[22] Y.Y. Gong, Y.Q. Tan, J. Mei, et al., Sci. China Chem. 56 (2013) 1178–1182.
[23] N. Jiang, D. Zhu, Z. Su, M.R. Bryce, Mater. Chem. Front. 5 (2021) 60–75.
[24] X. Zhao, P. Alam, J. Zhang, et al., CCS Chem. 4 (2022) 2570–2580.
[25] Z. Zhao, Z. Wang, J. Tavakoli, et al., Aggregate 2 (2021) e36.
[26] Y. Huang, J. Xing, Q. Gong, et al., Nat. Commun. 10 (2019) 169.
[27] Y. Hong, J.W.Y. Lam, B.Z. Tang, Chem. Soc. Rev. 40 (2011) 5361–5388.
[28] T. Han, D. Yan, Q. Wu, et al., Chin. J. Chem. 39 (2021) 677–689.
[29] Y. Hong, J.W.Y. Lam, B.Z. Tang, Chem. Commun. 29 (2009) 4332–4353.
[30] Y. Wang, X. Bin, X. Chen, et al., Macromol. Rapid Commun. 39 (2018) 1800528.
[31] R. Wang, W. Yuan, X. Zhu, Chin. J. Polym. Sci. 33 (2015) 680–687.
[32] X. Chen, W. Luo, H. Ma, et al., Sci. China Chem. 61 (2018) 351–359.
[33] H. Zhang, B.Z. Tang, JACS Au 1 (2021) 1805–1814.
[34] H. Zhang, Z. Zhao, P.R. McGonigal, et al., Mater. Today 32 (2020) 275–292.
[35] Q. Zhou, B. Cao, C. Zhu, et al., Small 12 (2016) 6586–6592.
[36] R. Hoffmann, Acc. Chem. Res. 4 (1971) 1–9.
[37] Q. Zhou, T. Yang, Z. Zhong, et al., Chem. Sci. 11 (2020) 2926–2933.
[38] Y.L. Wang, K. Chen, H.R. Li, et al., Chin. Chem. Lett. 34 (2023) 107684.
[39] B. Liu, H. Zhang, S. Liu, et al., Mater. Horiz. 7 (2020) 987–998.
[40] W. Luo, Y. Zhang, Y. Gong, et al., Chin. Chem. Lett. 29 (2018) 1533–1536.
[41] A. Pucci, R. Rausa, F. Ciardelli, Macromol. Chem. Phys. 209 (2008) 900–906.
[42] X. Chen, Y. Wang, Y. Zhang, W. Yuan, Prog. Chem. 31 (2019) 1560–1575.
[43] B. He, J. Zhang, J. Zhang, et al., Adv. Sci. 8 (2021) 2004299.

[44] Q. Huang, J. Cheng, Y. Tang, et al., Macromol. Rapid Commun. 42 (2021) 2100174.
[45] C. Shang, Y. Zhao, J. Long, Y. Ji, H. Wang, J. Mater. Chem. C 8 (2020) 1017–1024.
[46] C. Shang, N. Wei, H. Zhuo, et al., J. Mater. Chem. C 5 (2017) 8082–8090.
[47] C. Hu, Y. Ru, Z. Guo, et al., J. Mater. Chem. C 7 (2019) 387–393.
[48] Z. Guo, Y. Ru, W. Song, et al., Macromol. Rapid Commun. 38 (2017) 1700099.
[49] J. Deng, H. Jia, W. Xie, et al., Macromol. Chem. Phys. 223 (2022) 2100425.
[50] S. Tang, T. Yang, Z. Zhao, et al., Chem. Soc. Rev. 50 (2021) 12616–12655.
[51] Y. Wang, S. Tang, Y. Wen, et al., Mater. Horiz. 7 (2020) 2105–2112.
[52] S. Zheng, T. Zhu, Y. Wang, T. Yang, W.Z. Yuan, Angew. Chem. Int. Ed. 59 (2020) 10018–10022.
[53] Y. Lai, T. Zhu, T. Geng, et al., Small 16 (2020) 2005035.
[54] Y. Lai, Z. Zhao, S. Zheng, W. Yuan, Acta Chim. Sin. 79 (2021) 93–99.
[55] T. Zhu, T. Yang, Q. Zhang, W.Z. Yuan, Nat. Commun. 13 (2022) 2658.
[56] X. Ji, W. Tian, K. Jin, et al., Nat. Commun. 13 (2022) 3717.
[57] T. Yang, S. Dai, S. Yang, et al., J. Phys. Chem. Lett. 8 (2017) 3980–3985.
[58] J.S. Mohanty, K. Chaudhari, C. Sudhakar, T. Pradeep, J. Phys. Chem. C 123 (2019) 28969–28976.
[59] Z. Wu, Y. Du, J. Liu, et al., Angew. Chem. Int. Ed. 58 (2019) 8139–8144.
[60] X.H. Wu, P. Luo, Z. Wei, et al., Adv. Sci. 6 (2019) 1801304.
[61] X.L. Sun, D.M. Liu, D. Tian, et al., Nat. Commun. 8 (2017) 1210.
[62] Y.N. Jing, S.S. Li, M. Su, H. Bao, W.M. Wan, J. Am. Chem. Soc. 141 (2019) 16839–16848.
[63] S.S. Li, Y.N. Jing, H. Bao, W.M. Wan, Cell Rep. Phys. Sci. 1 (2020) 100116.
[64] S.S. Li, N. Zhu, Y.N. Jing, et al., iScience 23 (2020) 101031.
[65] M. Su, T. Li, Q.X. Shi, et al., Macromolecules 54 (2021) 9919–9926.
[66] Y.J. Sheng, M. Su, H. Xiao, et al., Chem. Eur. J. 28 (2022) e202201194.
[67] Q.X. Shi, Q. Li, H. Xiao, et al., Polym. Chem. 13 (2022) 592–599.
[68] Q.X. Shi, H. Xiao, Y.J. Sheng, et al., Polym. Chem. 13 (2022) 4524–4534.
[69] F. Huang, R.R. Hudgins, W.M. Nau, J. Am. Chem. Soc. 126 (2004) 16665–16675.
[70] A.E. Johnson, Traffic 6 (2005) 1078–1092.
[71] Z. Zhang, W. Yan, D. Dang, et al., Cell Rep. Phys. Sci. 3 (2022) 100716.
[72] Z. Zhang, Z. Zhang, H. Zhang, J.Z. Sun, B.Z. Tang, J. Polym. Sci. 60 (2022) 2127–2135.
[73] Q. Wen, Q. Cai, P. Fu, et al., Chin. Chem. Lett. 34 (2023) 107592.
[74] J. Ren, X. Shu, Y. Wang, et al., Chin. Chem. Lett. 33 (2022) 1650–1658.
[75] B. Chu, H. Zhang, K. Chen, et al., J. Am. Chem. Soc. 144 (2022) 15286–15294.